Anomalous Metal Phase Emergent on the Verge of an Exciton Mott Transition

Fumiya Sekiguchi, Toshimitsu Mochizuki, Changsu Kim, Hidefumi Akiyama, Loren N. Pfeiffer, Ken W. West, and Ryo Shimano

Phys. Rev. Lett. **118**, 067401 — Published 8 February 2017

DOI: 10.1103/PhysRevLett.118.067401

Anomalous metal phase emergent on the verge of exciton Mott transition

Fumiya Sekiguchi[1], Toshimitsu Mochizuki[2], Changsu Kim[2], Hidefumi Akiyama[2], Loren N. Pfeiffer[3], Ken W. West[3], and Ryo Shimano[1,4,*]

[1]*Department of Physics, The University of Tokyo, Tokyo, 113-0033, Japan*

[2]*Institute of Solid State Physics, The University of Tokyo, Kashiwa, 277-8581, Japan*

[3]*Department of Electrical Engineering, Princeton University, New Jersey 08544, USA*

[4]*Cryogenic Research Center, The University of Tokyo, Tokyo, 113-0032, Japan*

Abstract

We investigate the exciton Mott transition (EMT) by using optical pump-terahertz probe spectroscopy on GaAs, with realizing the condition of Mott's gedanken experiment by the resonant excitation of 1*s* excitons. We show that an anomalous metallic phase emerges on the verge of the EMT as manifested by peculiar enhancement of the quasiparticle mass and scattering rate. From the temperature and density dependence, the observed anomaly is shown to originate from the electron-hole (e-h) correlation which becomes prominent at low temperatures, possibly suggesting a precursor of e-h Cooper pairing.

PACS numbers: 71.30.+h, 71.35.-y, 71.45.Gm, 78.20.-e

Mott transition, i.e. insulator-to-metal transition (IMT) driven by the change of the inter-particle Coulomb interaction, is a fundamental phenomenon that appears widely in condensed matter systems such as doped semiconductors, correlated electron materials, and ultracold atom gases. It is highly suggestive that the global phase diagrams of such diverse systems have qualitatively similar features, and therefore the physics of Mott transition has been expected to provide comprehensive understandings on matter phases [1,2]. Among a variety of material systems, an ensemble of excitons, hydrogen-like bound electron-hole (e-h) pairs photoexcited in semiconductors, is one of the model systems that represents Mott's original argument on the IMT in an array of one-electron atoms [1]. The excitonic systems are unique playground in various aspects: 1) they are purely electronic, i.e. free from the influence of electron-lattice coupling, 2) long-range Coulomb interaction plays an essential role, and 3) the pair density can be precisely controlled by changing the photoexcitation intensity. When the e-h pair density increases and the mean inter-particle distance approaches to the exciton Bohr radius, insulating excitons dissociate into metallic free e-h plasma due to the screening of the Coulomb interaction, which results in the IMT termed as exciton Mott transition (EMT). One can find a close relation between EMT and Mott transition in the half-filled single-band Hubbard model, identifying the IMT in the latter case as the dissociation of bound doublons and holons [3,4]. EMT has long been investigated from the viewpoint of optoelectronic applications as well as of quantum many-body physics [5-14], nevertheless the fundamental nature of EMT remains unresolved. Mott suggested that at zero temperature the number of free charge carriers is discontinuous across the IMT and the transition has to be inherently first order. However, there has been a long debate whether IMT is first order or not in a continuous system like photoexcited e-h systems [15-22], with controversial experimental verifications [8-10,12-14].

Further intriguing problem of EMT is about the nature of electron correlation around the Mott transition. It is widely recognized that an anomalous metal phase emerges in the vicinity of the Mott transition in doped Mott insulators, and its relation to the peculiar electronic properties, e.g. high temperature superconducting phase and colossal magnetoresistance [2], has been intensively discussed. In e-h systems, however, the character of the metallic phase around the Mott transition remains elusive. The problem is also closely related to the theoretically anticipated quantum degenerate phases, i.e. exciton Bose-Einstein condensation and e-h BCS state, and the crossover between them [15,22-27]. The anticipated global phase diagram of e-h systems is schematically shown

in Fig. 1(a), though little is known about the low temperature electronic structures in the quantum degenerate regime.

To elucidate the intrinsic nature of EMT with representing the Mott's original argument, it is crucial to realize a sufficiently low temperature condition where all e-h pairs fall into the lowest 1*s* exciton state. In this Letter, we achieved such a condition by resonant photoexcitation of 1*s* excitons in a direct gap semiconductor GaAs, avoiding the photoinjection of excess energy into the system. To study the behavior of the e-h correlation around the EMT, we performed optical pump-terahertz probe (OPTP) spectroscopy which has been shown to be a powerful technique for the research of exciton formation dynamics and high density excitation phenomena including EMT in various semiconductors [11-14,28-31]. We show that an anomalous metal phase emerges in the vicinity of the EMT as manifested by the enhanced quasiparticle mass and scattering rate, which indicates the presence of non-vanishing e-h correlation in the metallic phase. Further, we investigate the formation dynamics of this anomalous correlation after the photoexcitation.

The schematic diagram of OPTP measurement is shown in Fig. 1(b). For a light source, we used a Ti:sapphire regenerative amplifier system. The terahertz (THz) probe pulse was generated from a GaP crystal and recorded using a ZnTe crystal. For the selective excitation of 1*s* excitons, the optical pump pulse was spectrally narrowed to the bandwidth of ~ 2.3 meV, and the pulse duration was ~ 2.1 ps. As a sample, we used a 1-μm-thick bulk GaAs, which is sandwiched by 1.7-μm-thick $Al_{0.18}Ga_{0.82}As$ spacer layers. The near-infrared optical density (OD) spectrum and the photoluminescence (PL) spectrum under the above-gap excitation are shown in Fig. 1(c), together with the optical pump spectrum for the 1*s* exciton-resonant excitation. Two sharp absorption peaks at 1.512 eV and 1.514 eV are assigned to the light-hole (lh) and heavy-hole (hh) 1*s* excitons, respectively [32]. The broad background tail below the 1*s* lh exciton line in the OD spectrum stems from the interference effect caused by the layered structure of the sample (See supplementary for details). The coincidence between the peak energies of the sharp PL and the absorption indicates that the sharp lines are those of free excitons. In this paper, we present the results obtained by the resonant excitation of 1*s* hh excitons, while similar results were obtained in the case of 1*s* lh exciton excitation. The complex dielectric function of the photoexcited e-h system is deduced from the

waveform of the transmitted electric-field (e-field) of the THz probe pulse [33]. Figure 1(d) shows one typical example of the photoinduced change of the real part of the optical conductivity $\Delta\sigma(\omega)$ and the dielectric function $\Delta\varepsilon(\omega)$ in the terahertz-frequency range, at pump-probe delay time t_{pp} = 10 ps and at relatively low pair density $n \sim 1.1\times10^{15}\,\mathrm{cm}^{-3}$. The intra-excitonic 1*s*-2*p* transition of free excitons is clearly observed at 3 meV as the peak structure in $\Delta\sigma(\omega)$ and the dispersive structure in $\Delta\varepsilon(\omega)$. Here, the spectera were taken with the attenuated THz probe pulse, 200 V/cm at the peak e-field, so that the linear response regime is ensured.

Figures 2(a,b) show the e-h pair density dependence of $\Delta\sigma(\omega)$ and $\Delta\varepsilon(\omega)$ at the lattice temperature $T_{lattice}$ = 5 K. The pump-probe delay is fixed at t_{pp} = 10 ps, before the heating of the e-h system occurs as we discuss later in detail. In the low density region the spectra are dominated by the 1*s*-2*p* intra-excitonic transition. As the density increases, the excitonic resonance becomes obscure and finally disappears. The overall monotonic spectral feature in the high density region seems to be those of metals, suggesting that the pair density reaches the metallic region above the EMT. The Mott density, which we define as the density where the excitonic structure disappears both in $\Delta\sigma(\omega)$ and $\Delta\varepsilon(\omega)$ spectra (the highest density in Figs. 2(a,b)), is estimated as $n_{\mathrm{Mott}} \sim 1.0\times10^{16}\,\mathrm{cm}^{-3}$. This value is close to the critical density $n_C \sim 1.3\times10^{16}\,\mathrm{cm}^{-3}$ given by the Mott's criteria [34], $n_C^{1/3} a_B = 0.26$, with the exciton Bohr radius of $a_B = 110$ Å in bulk GaAs. However, the spectra in this metallic region are not reproduced by the Drude model, which describes the charge carrier dynamcis of uncorrelated e-h plasma, as described in detail in the next paragraph. This fact makes a stark contrast with the data taken at high lattice temperetures where the spectra are well described by the Drude model, as shown in Figs. 2(e,f) for the case of 300 K. Here, in order to make the deviation from the Drude model in the low temperature regime tangible, we compare the spectra measured by weak THz probe (WTP) with those measured by strong probe THz pulses (STP), 3.2 kV/cm at the peak e-field, as shown in Figs. 2(c,d). At the low density of $n \sim 1.0\times10^{15}\,\mathrm{cm}^{-3}$, the excitonic 1*s*-2*p* transition resonance observed in the WTP spectrum completely disappears in the STP spectrum which is well reproduced by the Drude model. This spectral change is attributed to the dissociation of excitons into

free e-h plasma due to the strong e-field of the THz pulse [35]. We confirmed that the total spectral weight of $\Delta\sigma(\omega)$ is conserved between WTP and STP, which indicates that the total e-h pair density n is not changed by the STP pulse. Such a dependence of the spectra on the strength of the probe e-field was not observed at high temperatures where excitons are thermally ionized, as demonstrated again in Figs. 2(e,f). Therefore, the observed difference between WTP and STP spectra is attributed to the presence of excitonic e-h pair correlation which becomes dominant at low temperatures. Inversely, the difference between WTP and STP spectra can be used as an indicator for the presence of the excitonic correlation. Remarkably, the difference between WTP and STP spectra sustains even in the high density region, as shown in Figs. 2(c,d), revealing that the e-h correlation survives in the metal phase above the EMT. In this "correlated metal" (CM) phase, $\Delta\sigma(\omega)$ of the WTP exhibits a spectral weight transfer from lower to higher energy side compared to the STP case. Note that we evaluate n at each excitation densities from the Drude fits to the STP spectra using the reduced mass of e-h pairs, $m = (1/m_e + 1/m_h)^{-1} = 0.044 m_0$ (m_0 is the bare electron mass), having seen that the spectra taken by STP are well reproduced by the Drude model at all the excitation densities.

To gain a deeper insight into the nature of the observed CM phase above the EMT, we analized the WTP spectra using extended Drude model [42], in which the frequency-dependent complex scattering rate is introduced as $1/\tau = M(\omega) = 1/\tau(\omega) - i\omega\lambda(\omega)$. According to this model, the complex conductivity is described as

$$\sigma(\omega) = -\frac{1}{4\pi\varepsilon_0}\frac{Ne^2}{m^*(\omega)}\frac{1}{1-i\omega\tau^*(\omega)} \qquad (1)$$

where $m^*(\omega)/m = 1+\lambda(\omega)$ and $1/\tau^*(\omega) = (1+\lambda(\omega))/\tau(\omega)$. $m^*(\omega)/m$ and $1/\tau(\omega)$ are the frequency-dependent mass enhancement and scattering rate, respectively. Figures 3(a,b) show the density dependence of $m^*(\omega)/m$ and $1/\tau(\omega)$ spectra obtained from the analysis of the WTP spectra at t_{pp} = 10 ps. In the high density region

above n_{Mott}, $m^*(\omega)/m$ shows a clear enhancement towards the low energy region. Correspondingly, $1/\tau(\omega)$ exhibits a linear increase towards the high energy side. For comparison, $m^*(\omega)/m$ and $1/\tau(\omega)$ spectra obtained with STP at the highest density are also plotted as broken lines in Figs. 3(a,b), which do not show such frequency dependence, reaffirming that the STP spectra are well described by the simple Drude model. Figures 3(c,d) show the lattice temperature dependence of $m^*(\omega)/m$ and $1/\tau(\omega)$ at the highest density $n \sim 3.0\times10^{16}\,\mathrm{cm}^{-3}$. The characteristic of the CM phase as manifested by the frequency-dependent $m^*(\omega)/m$ and $1/\tau(\omega)$ is identified up to ~ 40 K, but fades away above 60 K. Considering the Bose factor of the optical phonon in GaAs existing at 36 meV, the phonon population steeply increases around 60 K. Thus the disappearance of the CM phase is attributed to the rapid heating of the e-h system due to the optical phonon absorption. Importantly, when the lattice temperature raises the scattering rate $1/\tau(\omega)$ *decreases* and becomes frequency independent. These observations indicate that the anomalous enhancement of the mass and the scattering rate originates from the e-h Coulomb correlation that becomes prominent at low temperatures. It should be noted here that the Fermi-Liquid theory in the degenerate regime also predicts the frequency-dependent scattering rate due to the Pauli blocking effect [43], while it expects suppression but not enhancement of the low energy intraband scattering rate, which is opposite to the experimental result. Therefore, the emergence of the CM phase is most likely regarded as the anomalous metal phase that is known to appear on the verge of Mott transition [2]. It is worth noting that, even without resorting to the above quasiparticle picture, the modification of the spectral function due to e-h correlations has been theoretically argued in terms of a precursor of e-h Cooper pairing [15,20,24] in the same density region as the present experiment.

Next we show how the CM phase evolves over time after the photoexcitation. To grasp the signature of the CM clearly, we plot the differential optical conductivity spectra $\Delta(\Delta\sigma(\omega))$ by subtracting STP $\Delta\sigma(\omega)$ from WTP $\Delta\sigma(\omega)$. Figure 4(a) shows the density dependence of $\Delta(\Delta\sigma(\omega))$ at t_{pp} = 10 ps. In the low density region, 1*s* exciton population gives a positive peak around 3 meV in $\Delta(\Delta\sigma(\omega))$, whereas in the high density CM phase $\Delta(\Delta\sigma(\omega))$ spectra show negative values in the low energy region reflecting the spectral

weight transfer from lower to higher energy side in $\Delta\sigma(\omega)$. Therefore, we can discuss the dynamics of the e-h correlation from the temporal evolution of $\Delta(\Delta\sigma(\omega))$ in the low energy region as indicated in Fig. 4(a). The results at various photoexcitation densities are shown in Fig. 4(b). At the lowest density of $n \sim 1.2\times10^{15}\,\mathrm{cm}^{-3}$, a step-like positive signal appears right after the photoexcitation and remains constant over the observation range of 75 ps. This behavior is simply interpreted that the population of photo-created 1*s* excitons remains nearly constant in the observed temporal range since excitons have much longer lifetime (>1 ns) [44]. As the density increases and approaches to n_{Mott}, a peculiar behavior emerges: the signal decreases over time after the photoexcitation. The decrease of the signal, which corresponds to the formation of the CM phase, becomes prominent and faster at the higher density region, suggesting the stability of the CM phase at higher densities (see Fig. 4(e)). After reaching the maximum value, the CM decays in a relatively long timescale. The $\Delta(\Delta\sigma(\omega))$ spectra taken at longer time delay, where the CM phase no more exists, are similar to those obtained with the nonresonant excitation at 8 meV above the band edge (compare the spectra in Figs. 4(c,d)). Considering that the CM phase appears only under the resonant excitation of 1*s* excitons at low lattice temperatures, the decay dynamics of the CM observed in Fig. 4(b) is attributed to the heating of the e-h system, presumably caused by the nonradiative e-h recombination, likely the Auger process [45]. A closer inspection to the formation dynamics of the CM phase in Fig. 4(b) implies the existence of an incubation time at the intermediate density range near n_{Mott}, marked by double-headed arrows. Such a presence of incubation time is reported in the quench dynamics of the first-order phase transition in certain systems [46]. Incubation time is sometimes related to the cooperative phenomena in a system, if there exists a positive feedback in the phase transition [46-48]. In e-h systems, screening effect of the Coulomb interaction and stability of excitons are mutually dependent: excitons are more destabilized as unbound e-h pairs increase through the exciton ionization, and such a feedback effect has been discussed in relation to a first-order EMT accompanied by a bistability at low temperatures [18-21]. In general, temporal evolution of the system becomes slower around the edge of the bistable region [48], and the incubation time in the CM

formation may indicate such a signature of the first-order transition from oversaturated exciton gas to CM. It is an important problem whether the EMT is accompanied by intrinsic spatial inhomogeneity, e. g., due to the formation of e-h droplets (EHDs) [49]. However, EHDs in GaAs are expected to be unstable [17,50], and indeed the surface plasmon resonance of EHDs, which should appear in the observation frequency range if EHDs exist, was not observed.

To summarize, we investigated the EMT in bulk GaAs under the resonant photoinjection of 1*s* excitons by OPTP spectroscopy. An anomalous metallic phase, characterized by the peculiar quasiparticle mass enhancement and scattering rate, was discovered on the verge of the EMT. Considering that the anomaly in the present case is caused by the e-h Coulomb correlation, the correlated metal phase emergent only at low temperature region may be viewed as a precursor of e-h BCS state [15,20,23,24]. The experimental verification of such a new quantum matter phase has long been explored, and the present ultrafast spectroscopic scheme to extract sensitively the e-h correlation would be promising for further future investigations.

We thank K. Asano for illuminating discussions and T. Ogawa for valuable comments. The work at The University of Tokyo was supported by a Grant-in-Aid for Scientific Research (Grant No. 22244036 and 15H02102). The work at Princeton University was funded by the Gordon and Betty Moore Foundation through the EPiQS initiative Grant GBMF4420, and by the National Science Foundation MRSEC Grant DMR-1420541.

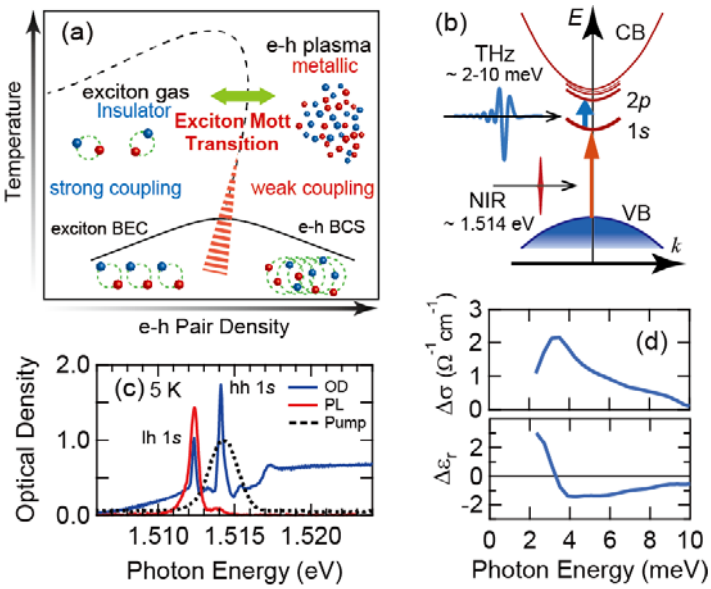

FIG. 1 (a) Schematic phase diagram of e-h systems in photoexcited semiconductors. (b) Energy diagram of our OPTP measurement. (c) Solid blue line: near-infrared optical density spectrum of the sample around the band edge. Solid red line: photoluminescence spectrum under the above-gap excitation condition. Dashed line: spectrum of the optical pump. (d) Photoinduced changes of the real part of (top panel) optical conductivity $\Delta\sigma(\omega)$ and (bottom panel) dielectric function $\Delta\varepsilon(\omega)$.

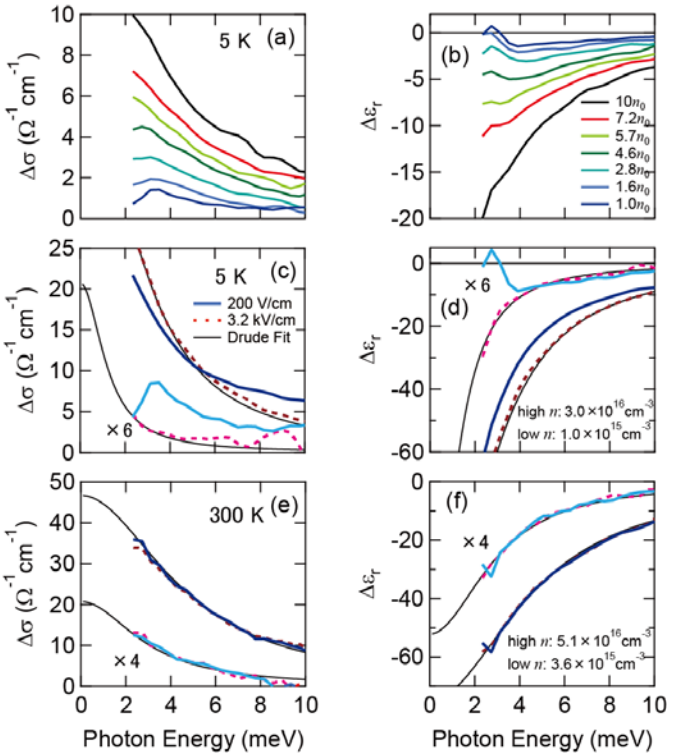

FIG. 2 (a,b) Pair density dependence of (a) $\Delta\sigma(\omega)$ and (b) $\Delta\varepsilon(\omega)$ spectra obtained with the weak THz probes at t_{pp} = 10 ps, from $1.0n_0$ to $10n_0$ with $n_0 = 1.0\times10^{15}\,\mathrm{cm}^{-3}$. (c,d) Comparison of the weak and the strong THz probe spectra of (c) $\Delta\sigma(\omega)$ and (d) $\Delta\varepsilon(\omega)$ at T_{lattice} = 5 K, at the low density $1.0\times10^{15}\,\mathrm{cm}^{-3}$ and the high density $3.0\times10^{16}\,\mathrm{cm}^{-3}$. The spectra taken by weak (strong) THz probe pulse are shown as solid (dashed) lines, and thin black solid lines are the fitted result of strong THz probe spectra with the Drude model. (e,f) Comparison of the weak and the strong THz probe spectra of (e) $\Delta\sigma(\omega)$ and (f) $\Delta\varepsilon(\omega)$ at t_{pp} = 10 ps and at T_{lattice} = 300 K.

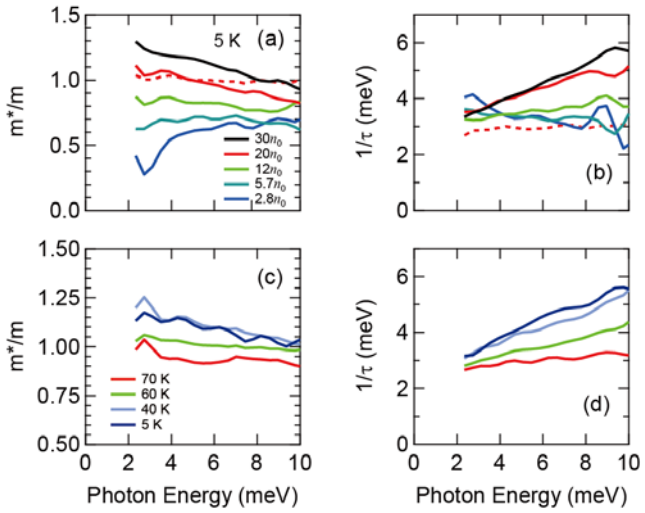

FIG. 3 (a,b) Pair density dependence of (a) quasiparticle mass enhancement $m^*(\omega)/m$ and (b) scattering rate $1/\tau(\omega)$ spectra, from $2.8n_0$ to $30n_0$ with $n_0 = 1.0\times10^{15}\,\mathrm{cm}^{-3}$. Dashed lines correspond to the spectra at $30n_0$ taken with the strong THz probe. (c,d) Temperature dependence of (c) $m^*(\omega)/m$ and (d) $1/\tau(\omega)$ spectra.

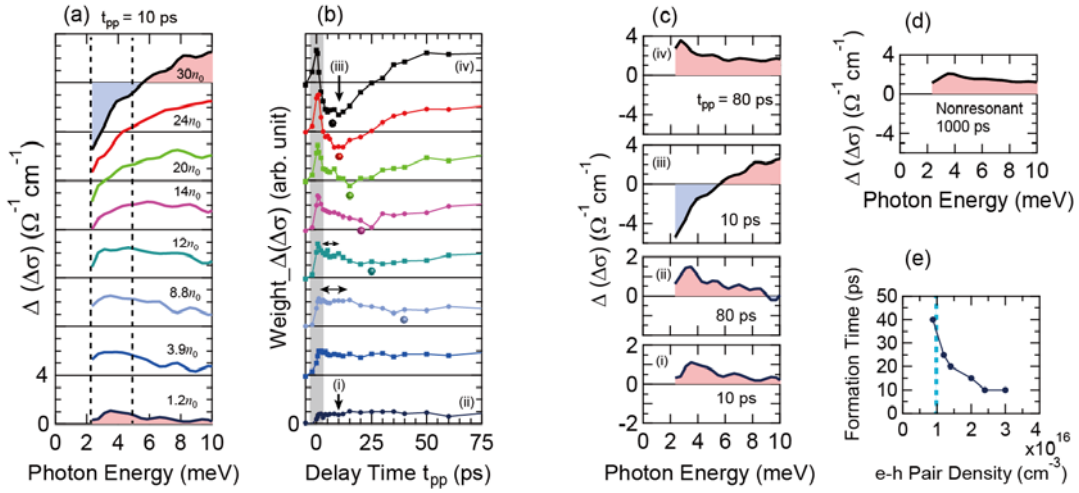

FIG. 4 (a) Differential optical conductivity spectra $\Delta(\Delta\sigma(\omega))$ at t_{pp} = 10 ps at different densities. (b) Spectral weight dynamics of the $\Delta(\Delta\sigma(\omega))$ integrated in the region between the dashed lines in Fig. 4(a). The gray-shaded area indicates the region where the pump and probe pulses temporally overlaps. (c) $\Delta(\Delta\sigma(\omega))$ spectra at the lowest (i and ii) and the highest (iii and iv) density, at t_{pp} = 10 ps (i and iii) and 80 ps (ii and iv), indicated in Fig. 4(b). (d) $\Delta(\Delta\sigma(\omega))$ spectrum under the condition of nonresonant excitation (~ 8 meV above the band edge) at high density $2.7\times10^{16}\,\mathrm{cm}^{-3}$ and at t_{pp} = 1000 ps, which corresponds to the quasi-thermal equilibrium condition at T ~ 5 K. (e) The density dependence of the formation time of the CM. Dashed line indicates n_{Mott}.

References

*shimano@phys.s.u-tokyo.ac.jp

[1] N. F. Mott, Philosophical Magazine **6**, 287 (1961).

[2] M. Imada, A. Fujimori, and Y. Tokura, Reviews of Modern Physics **70**, 1039 (1998).

[3] M. Imada, Physical Review B **72**, 075113 (2005).

[4] H. Yokoyama, M. Ogata, and Y. Tanaka, Journal of the Physical Society of Japan **75**, 114706 (2006).

[5] H. Haug and S. Schmitt-Rink, Progress in Quantum Electronics **9**, 3 (1984).

[6] G. W. Fehrenbach, W. Schäfer, J. Treusch, and R. G. Ulbrich, Physical Review Letters **49**, 1281 (1982).

[7] Y. Hayamizu, M. Yoshita, Y. Takahashi, H. Akiyama, C. Z. Ning, L. N. Pfeiffer, and K. W. West, Physical Review Letters **99**, 167403 (2007).

[8] L. M. Smith and J. P. Wolfe, Physical Review Letters **57**, 2314 (1986).

[9] L. Kappei, J. Szczytko, F. Morier-Genoud, and B. Deveaud, Physical Review Letters **94**, 147403 (2005).

[10] M. Stern, V. Garmider, V. Umansky, and I. Bar-Joseph, Physical Review Letters **100**, 256402 (2008).

[11] R. A. Kaindl, M. A. Carnahan, D. Hagele, R. Lovenich, and D. S. Chemla, Nature **423**, 734 (2003).

[12] R. Huber, R. A. Kaindl, B. A. Schmid, and D. S. Chemla, Physical Review B **72**, 161314 (2005).

[13] T. Suzuki and R. Shimano, Physical Review Letters **109**, 046402 (2012).

[14] F. Sekiguchi and R. Shimano, Physical Review B **91**, 155202 (2015).

[15] R. Zimmermann and H. Stolz, physica status solidi (b) **131**, 151 (1985).

[16] L. D. Landau and G. Zeldovich, Acta Phys. Chim. USSR **18**, 194 (1943).

[17] J. C. Hensel, T. G. Phillips, T. M. Rice and G. A. Thomas, *Solid State Physics* (ACADEMIC PRESS, 1977)

[18] I. Balslev, Solid State Communications **27**, 545 (1978).

[19] D. W. Snoke and J. D. Crawford, Physical Review E **52**, 5796 (1995).

[20] K. Asano and T. Yoshioka, Journal of the Physical Society of Japan **83**, 084702 (2014).

[21] D. Semkat, F. Richter, D. Kremp, G. Manzke, W. D. Kraeft, and K. Henneberger, Physical Review B **80**, 155201 (2009).

[22] T. Ogawa, Y. Tomio and K. Asano, Journal of Physics: Condensed Matter **19**, 295205 (2007).

[23] L. V. Keldysh and Y. V. Kopaev, SOVIET PHYSICS SOLID STATE,USSR **6**, 2219 (1965).

[24] R. Zimmermann, physica status solidi (b) **86**, K63 (1978).

[25] P. Nozières and S. Schmitt-Rink, J. Low Temp. Phys. **59**, 195 (1985).

[26] D. Jérome, T. M. Rice, and W. Kohn, Physical Review **158**, 462 (1967).

[27] A. Griffin, D. W. Snoke, and S. Stringari, *Bose-Einstein Condensation* (Cambridge University Press, 1996).

[28] S. W. Koch, M. Kira, G. Khitrova, and H. M. Gibbs, Nat. Mater. **5**, 523 (2006).

[29] M. Kira and S. W. Koch, Progress in Quantum Electronics **30**, 155 (2006).

[30] T. Suzuki and R. Shimano, Physical Review Letters **103**, 057401 (2009).

[31] R. Ulbricht, E. Hendry, J. Shan, T. F. Heinz, and M. Bonn, Reviews of Modern Physics **83**, 543 (2011).

[32] M. Nakayama, T. Doguchi and H. Nishimura, J. Appl. Phys. **72**, 2372 (1992)

[33] R. A. Kaindl, D. Hägele, M. A. Carnahan, and D. S. Chemla, Physical Review B **79**, 045320 (2009).

[34] P. P. Edwards and M. J. Sienko, Physical Review B **17**, 2575 (1978).

[35] See Supplemental Material [url], which includes Refs. [36-41]

[36] B. Zaks, R. B. Liu, and M. S. Sherwin, Nature **483**, 580 (2012).

[37] B. Ewers *et al*., Physical Review B **85**, 075307 (2012).

[38] F. Langer *et al*., Nature **533**, 225 (2016).

[39] Y. Mukai, H. Hirori, and K. Tanaka, Physical Review B **87**, 201202 (2013).

[40] H. Hirori, K. Shinokita, M. Shirai, S. Tani, Y. Kadoya, and K. Tanaka, Nat. Commun. **2**, 594 (2011).

[41] A. Dargys and S. Zurauskas, J. Phys.: Condens. Matter **7**, 2133 (1995).

[42] D. N. Basov and T. Timusk, Reviews of Modern Physics **77**, 721 (2005).

[43] N. W. Ashcroft and N. D. Mermin, *Solid State Physics* (Holt, Rinehart and Winston, 1976)

[44] G. W. 't Hooft, W. A. J. A. van der Poel, L. W. Molenkamp, and C. T. Foxon, Physical Review B **35**, 8281(R) (1987).

[45] M. C. Downer and C. V. Shank, Physical Review Letters **56**, 761 (1986)

[46] Y. Ogawa, S. Koshihara, K. Koshino, T. Ogawa, C. Urano, and H. Takagi, Physical Review Letters **84**, 3181 (2000).

[47] H. Gomi, T. Kawatani, T. J. Inagaki, and A. Takahashi, Journal of the Physical Society of Japan **83**, 094714 (2014).

[48] K. Koshino and T. Ogawa, Journal of the Physical Society of Japan **68**, 2164 (1999).

[49] C. D. Jeffries and L. V. Keldysh, *Electron-hole droplets in semiconductors* (North-Holland, 1983).

[50] W. F. Brinkman and T. M. Rice, Physical Review B **7**, 1508 (1973).